

Cosmological neutrino mass limits: variations with choice of data sets and a new, bias-free limit

Jostein R. Kristiansen,* Øystein Elgarøy,† and Håkon Dahle‡

Institute of Theoretical Astrophysics, University of Oslo, Box 1029, 0315 Oslo, NORWAY

(Dated: December 2, 2024)

We discuss the variation of cosmological upper bounds on M_ν , the sum of the neutrino masses, with the choice of data sets included in the analysis, pointing out a few oddities not easily seen when all data sets are combined. For example will the effect of applying different priors vary significantly depending on whether we use large scale structure data from the 2dF or SDSS galaxy survey. We argue that this can be explained by inconsistencies between these two data sets. A conservative neutrino mass limit of $M_\nu < 1.43\text{eV}$ (95% C.L.) is obtained by combining the WMAP 3 year date with the cluster mass function measured by weak gravitational lensing. This limit has the virtue of not making any assumptions about the bias of luminous matter with respect to the dark matter.

I. INTRODUCTION

The fact that neutrinos undergo flavour oscillations, implying that not all neutrinos are massless, is one of the most important discoveries in particle physics in the last decade. Oscillations are only sensitive to the mass-squared differences between the neutrino mass eigenstates (see e.g. [1, 2]), and although these are suggestive of the overall mass scale, they cannot pin the absolute mass scale firmly. For that, one needs probes like tritium beta decay [3] or neutrinoless double beta decay [4]. At the moment, however, the strongest upper bound on the neutrino mass scale comes from cosmology (see e.g. [5, 6]). The cosmological mass limits are based on the implications of neutrino masses for clustering of matter, in particular the fact that neutrinos can free-stream out of density perturbations and impede structure formation on small scales if they are a significant fraction of the dark matter. For a thorough review, see [7].

Impressive as they are, the cosmological neutrino mass limits involve several assumptions. First of all, they assume that the underlying cosmological model is of the Friedmann-Robertson-Walker type, that gravity is described by general relativity, the primordial power spectrum of density perturbations is a scale-free power-law, and that the dark energy is a cosmological constant. Modifications of this simple picture have been considered [8], and in particular the degeneracy between neutrino masses and the dark energy equation of state has been investigated in some recent papers [5, 9, 10, 11, 12]. Secondly, the upper limit depends on the cosmological data sets used in the analysis. It is this last aspect of the problem we will consider in the present paper, working within the context of the standard Λ CDM paradigm.

The angular power spectrum of the temperature anisotropies in the cosmic microwave background (CMB) radiation is generally considered to be the cleanest cos-

mological data set. Unfortunately the CMB cannot provide upper limits on M_ν better than $\sim 1.6\text{ eV}$ [13], which is almost reached already now with the WMAP 3-year data [14, 15, 16]. An improvement of this limit requires some probe of the matter distribution. The most common probe is the power spectrum of the galaxy distribution, as determined by large redshift surveys like the 2 degree Field Galaxy Redshift Survey (2dFGRS) [17] and the Sloan Digital Sky Survey (SDSS) [18]. The distribution of the galaxies is biased with respect to that of the dark matter, but if the bias is independent of length scale, this is not a serious limitation. However, recent results suggest that the story of bias might be more complicated than the simple assumption of scale-independent bias that has gone into earlier cosmological mass limits [19, 20].

Ideally, one would like to rely on probes that are sensitive to the total matter distribution. One such probe is measurements of weak gravitational lensing by matter along random lines of sight [21, 22]. However, even the most ambitious of these 'cosmic shear' surveys have covered less than one percent of the full sky, thus probing only a limited cosmological volume. A somewhat different approach is to count the number of rare, high density peaks in the matter fluctuations within a larger volume. These peaks correspond to very massive clusters of galaxies, their abundances (the so-called cluster mass function) being highly sensitive to the amplitude of the matter power spectrum (see e.g. [23] and references therein) on corresponding scales. Until recently, cluster masses were generally derived based on observables of the baryonic mass component, such as the temperature of the X-ray emitting intra-cluster medium (ICM). In this case, one had to calibrate the X-ray temperature-mass relationship, either from simulations or from observational mass measurements relying on assumptions about hydrostatical equilibrium of the ICM. However, [24] provided for the first time a measurement of the cluster mass function (CMF) where the cluster masses have been established directly by weak gravitational lensing. The main result of this paper is an upper bound on the sum of the neutrino masses obtained by combining the WMAP 3-year

*Electronic address: j.r.kristiansen@astro.uio.no

†Electronic address: oelgaroy@astro.uio.no

‡Electronic address: hakon.dahle@astro.uio.no

data with the CMF derived by Dahle [24]. Although not as impressive as e.g. the limit obtained by combining all available cosmological observations, including the Lyman alpha forest power spectrum, this limit is robust in the sense that it makes use of clean cosmological probes, and involves a minimum of assumptions.

II. MASSIVE NEUTRINOS IN COSMOLOGY

We work within the standard cosmological paradigm of the Λ CDM model, and leave studies of significant deviations from this model for a future study. Our adopted notation is as follows: We denote as Ω_i the present density of component i in units of the density of a spatially flat universe. Note that Ω_m is the total density of all non-relativistic components, so that $\Omega_m = \Omega_{CDM} + \Omega_b + \Omega_\nu$, with Ω_b being the present baryon density. The density parameter Ω_ν is determined by the sum of the neutrino masses M_ν and the present value of the Hubble parameter $H_0 = 100h \text{ km s}^{-1} \text{ Mpc}^{-1}$ [25]:

$$\Omega_\nu h^2 = \frac{M_\nu}{93.14 \text{ eV}}. \quad (1)$$

As we will see, present cosmological probes (with the possible exception of the Lyman alpha forest [6]) are only sensitive to neutrino masses larger than a few tenths of an eV. In this regime, the neutrino mass spectrum would be degenerate, and hence $M_\nu = 3m_\nu$, where m_ν is the common mass of the neutrino mass eigenstates.

Within the Λ CDM model the effect of massive neutrinos on structure formation is simple. Their influence on structure formation is governed mainly by the quantity $f_\nu = \Omega_\nu/\Omega_m$. While relativistic, the neutrinos free-stream out of density perturbations on scales smaller than the Hubble radius. Once they become non-relativistic, the free-streaming scale is set by their root-mean-square velocity. The maximum length scale below which all scales are affected by neutrino free-streaming is thus set by the horizon size when the neutrinos became non-relativistic. This quantity is given by [7]

$$\begin{aligned} k_{nr} &= 0.018 \left(\frac{m_\nu}{1 \text{ eV}} \right)^{1/2} \Omega_m^{1/2} h \text{ Mpc}^{-1} \\ &= 0.1 f_\nu^{1/2} \Omega_m h \text{ Mpc}^{-1}. \end{aligned} \quad (2)$$

Note that the combination $\Omega_m h$ enters this expression; this quantity determines the Hubble radius at matter-radiation equality and is an important length scale in the power spectrum of matter density fluctuations. This scale is similar to the neutrino free-streaming scale: below this scale, density perturbations are suppressed. Hence, there is a degeneracy between $\Omega_m h$ and f_ν .

For scales below the neutrino free-streaming scale, $k > k_{nr}$, the main effect is a reduction by a factor $1 - f_\nu$ of the source term in the equation for the linear growth of density perturbation. Hence, the amount of suppression is also set by the parameter f_ν , and so it

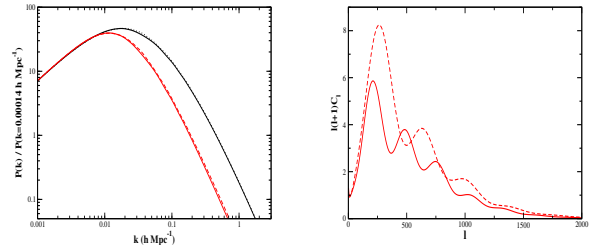


FIG. 1: Illustration of how combining data sets break degeneracies. The left panel shows the matter power spectrum in four different models, where the baryon density has been artificially set low and a scale invariant power spectrum of adiabatic primordial perturbations has been assumed. The black lines are for models with $\Omega_\nu = 0$. The full line has $\Omega_m = 0.25$ and $h = 0.735$, whereas the dashed line has $\Omega_m = 0.50$ and $h = 0.3675$. The red lines are models with massive neutrinos. The full line has $\Omega_m = 0.25$, $\Omega_\nu = 0.05$ and $h = 0.735$, and the dashed line has $\Omega_m = 0.50$, $\Omega_\nu = 0.10$ and $h = 0.3675$. Note that $f_\nu = 0.2$ in both cases. The right panel shows the CMB power spectra for the two models with massive neutrinos, with the same line coding. The models have very different CMB power spectra, and hence measurements of the CMB anisotropies help constraining Ω_ν .

is this, and not M_ν which is directly accessible in measurements of large-scale structure. Since we can write $M_\nu = 93.14 f_\nu \Omega_m h^2 \text{ eV}$, we see that one also needs a constraint on $\Omega_m h^2$ to go from a limit on f_ν to a limit on M_ν . Figure 1 illustrates this situation in a toy example. It is seen that the matter power spectrum must be combined with other probes, for example the CMB power spectrum, in order to provide stringent constraints on M_ν .

III. DATA AND METHODS

In our analysis we have used data from both CMB, observations of large scale structures (LSS), type Ia supernovae (SNIa), baryon acoustic oscillations (BAO), and additional priors on the Hubble parameter and the baryon content of the universe. We have also applied constraints on the cluster mass function from weak gravitational lensing.

A. CMB data

The 3-year data release from the WMAP team [26] is at present the most constraining set of CMB observations. The WMAP experiment is a full-sky survey of CMB temperature anisotropies. With this release, a Fortran 90 code for calculating the likelihood of a given CMB power spectrum against the data was also provided. However, in ref. [27] it was noted that this likelihood code applied a sub-optimal likelihood approximation on large scales

($l \lesssim 30$), and in ref. [28] the authors pointed out an over-subtraction of unresolved point sources on small angular scales ($l \gtrsim 30$). Correcting for these two effects resulted in a slight shift in some cosmological parameter values. In ref. [16], it was shown that these corrections to the WMAP likelihood code also shifted the upper limit on the neutrino masses from $M_\nu < 1.90\text{eV}$ to $M_\nu < 1.57\text{eV}$ when using WMAP data only. In a revised version of the WMAP likelihood code[43], these corrections have to some extent been accounted for, and the results using this code is in better agreement with refs. [16, 28] than the previous version. In this paper we will make use of this revised likelihood code from the WMAP team. We note, however, that the upper limits on M_ν would have been slightly lower with the code used in refs. [16, 28].

In this work we are not considering CMB data from other experiments than WMAP, since we want to restrict the number of data sets as much as possible, and since these additional data sets have been shown not to improve the limits on M_ν [16].

B. Large scale structure

Large scale structure surveys probe the matter distribution in the universe by measuring the galaxy-galaxy power spectrum $P_g(k, z) = \langle |\delta_g(k, z)|^2 \rangle$. Since massive neutrinos give a distinct imprint on the LSS due to their free-streaming effect, data from galaxy surveys have proven to be important to put tight constraints on neutrino masses. However, such surveys are also troubled by bias effects that are hard to quantify. For example, it is assumed that in the linear perturbation regime, the total matter power spectrum, P_m , is proportional to the galaxy power spectrum by the simple relation $P_g = b^2 P_m$. Recently, the use of this simple relation has been debated [19, 20], and it is at present unclear how important the corrections for a scale-dependent b might be.

There are two galaxy surveys of comparable size, the 2 degree Field Galaxy Redshift Survey (2dF) [17], and the Sloan Digital Sky Survey (SDSS) main sample [29]. As has been pointed out in e.g. [19, 30, 31], there is some tension between the results from 2dF and SDSS. As a relevant example for this paper, the combination SDSS+WMAP prefers larger values of both Ω_m and σ_8 (the rms mass fluctuations in spheres of radius $8h^{-1}$ Mpc) than what is found when using data from 2dF+WMAP. In a recent analysis of the 2dF+SDSS discrepancy [31], the authors conclude that it is caused by non-linear bias effects. They also claim that SDSS is more sensitive to these effects than the 2dF sample, since the SDSS sample contains more red galaxies, which are believed to cluster slightly different from blue galaxies.

Regardless of their origin, the reported inconsistencies between the 2dF and SDSS galaxy surveys tell us that we should always be cautious when including LSS data in our parameter estimation, at least until the scale dependence of the bias parameter is better understood.

C. Type Ia supernovae

The luminosity distance-redshift relationship measured by observations of supernovae of type Ia (SNIa) provides the most direct evidence for cosmic acceleration and dark energy. There are still open questions regarding both the exact mechanism behind these supernovae and their use as ‘standard candles’, and so we choose not to rely on SNIa in our robust neutrino mass limit. When we do use them, we use the data from the Supernova Legacy Survey (SNLS) [32].

D. The cluster mass function

Massive galaxy clusters are extremely rare high-density peaks in the matter fluctuations, containing matter originating from a co-moving volume spanning $\sim 10h^{-1}$ Mpc which has undergone gravitational collapse. Their abundances, as quantified by the CMF, are thus a sensitive probe of σ_8 and Ω_m . While all previous measurements of the CMF have been based on observations of baryonic tracers of cluster mass (with inherent uncertainties and possible biases which are not yet fully understood; see e.g. [33]), the CMF of [24] was derived from weak gravitational lensing measurements of the masses of a volume-limited sample of X-ray luminous clusters. The details of the data reduction and weak gravitational shear estimator are given in [34], and [24] describes the derivation of cluster masses from gravitational lensing measurements. The cluster sample of [24] was selected from a large volume of $8.0 \times 10^8 (h^{-1}\text{Mpc})^3$ (assuming a spatially flat universe with $\Omega_m = 0.3$), above a threshold value in X-ray luminosity (L_X). Using L_X as a proxy for mass in the cluster selection could in principle introduce a baryonic bias to the CMF measurements, depending on L_X measurement uncertainties and the intrinsic scatter around the mass- L_X relation. In [24], any such effects were effectively removed, by carefully calibrating the amplitude of the mass- L_X relation and the scatter around the mean relation (thereby estimating the sample completeness as a function of mass), and by calculating cosmological parameter constraints exclusively based on the clusters well above the mass threshold corresponding to the X-ray luminosity threshold of the sample (where the sample is virtually complete).

Parameter constraints in the $\sigma_8 - \Omega_m$ plane were obtained by fitting the observed cluster abundances in three mass intervals to theoretical predictions for the CMF [35]. We have found that the value of χ^2 from the CMF from [24] can be approximated by the fit-function

$$\chi^2_{\text{CMF}} = 10000u^4 + 6726u^3 + 1230u^2 - 4.09u + 0.004, \quad (3)$$

where $u = \sigma_8(\Omega_m/0.3)^{0.37} - 0.67$.

E. Other priors

We have also tested the sensitivity of neutrino mass limits on priors from the Hubble Space Telescope Key Project on the Extragalactic Distance Scale (HST), and Big Bang nucleosynthesis (BBN) predictions.

From HST, we use a prior on the Hubble parameter of $h = 0.72 \pm 0.08$ [36], and from BBN we use a prior on the physical baryon density today, $\Omega_b h^2 = 0.020 \pm 0.002$ [37]. There are hints of some tension between the WMAP constraint on $\Omega_b h^2$ and the value of this quantity inferred from the ${}^4\text{He}$ abundance [38], so in our robust limit we will not use the BBN prior. Since there is still some debate about the value of the Hubble constant derived from the HST Key Project [39, 40], we also drop this prior when deriving our robust limit.

We have also added information on the position of the baryonic acoustic oscillation (BAO) peak in the luminous red galaxy (LRG) sample in the SDSS survey [41]. This prior is implemented by an effective fit function as described in [5]. Using an effective parameter

$$A_{\text{BAO}} = \left[D_M(z)^2 \frac{z}{H(z)} \right]^{1/3} \frac{\sqrt{\Omega_m H_0^2}}{z}, \quad (4)$$

where $D_M(z)$ is the comoving angular diameter distance, the authors impose the constraint

$$A_{\text{BAO}} = 0.469 \left(\frac{n_s}{0.98} \right)^{-0.35} (1 + 0.94 f_\nu) \pm 0.017. \quad (5)$$

Throughout our analysis we have also applied a top-hat prior on the age of the universe, $10\text{Gyr} < \text{Age} < 20\text{Gyr}$.

F. Parameter estimation

For the parameter estimations we have used the publicly available Markov chain Monte Carlo code CosmoMC [42]. We have used a basic seven-parameter model, varying the parameters $\{\Omega_b h^2, \Omega_m, \log(10^{10} A_S), h, n_s, \tau, M_\nu\}$. M_ν is defined in eq. (1). For the other parameters, the exact definitions are given by the CosmoMC code. We have assumed spatial flatness, no running of the scalar spectral index, that the dark energy is a cosmological constant and that the tensor to scalar fluctuation amplitude is negligible. These assumptions are well motivated by current available data [14]. Also, adding these extra degrees of freedom do not affect the limits on M_ν drastically [16].

Often cosmological neutrino mass limits are found using a large number of different data sets and priors simultaneously. In this analysis we consider in total 48 different combinations of data sets and priors to see how the different data sets alter the neutrino mass limit.

IV. RESULTS

The neutrino mass limits found in our analysis are summarized in Table I. The limits quoted in the table range from $M_\nu \lesssim 6\text{eV}$ from using LSS data only, via $M_\nu < 1.75\text{eV}$ from WMAP data only, and down to $M_\nu < 0.40\text{eV}$ for a combination of WMAP, SDSS, SNLS BAO and HST data.

Data set	no prior	CMF	HST	BBN
WMAP	1.75eV	1.43eV	1.47eV	1.73eV
WMAP+2dF	1.02eV	0.89eV	0.92eV	1.01eV
WMAP+SDSS	1.05eV	1.13eV	0.87eV	1.05eV
WMAP+SNLS	1.10eV	0.70eV	1.02eV	1.07eV
SDSS	5.8eV	4.6eV	6.1eV	6.0eV
2dF	5.2eV	5.3eV	5.3eV	5.2eV
WMAP+2dF+SNLS	0.81eV	0.64eV	0.76eV	0.80eV
WMAP+SDSS+SNLS	0.44eV	0.57eV	0.42eV	0.44eV
WMAP+2dF+SNLS+BAO	0.84eV	0.69eV	0.79eV	0.84eV
WMAP+SDSS+SNLS+BAO	0.42eV	0.56eV	0.40eV	0.42eV
WMAP+SDSS+BAO	0.55eV	0.76eV	0.52eV	0.56eV
WMAP+2dF+BAO	1.04eV	0.89eV	0.92eV	1.01eV

TABLE I: Estimated 95% C.L. upper limits on M_ν . The CMF, HST and BBN priors are added one at the time to the combination of data sets given in the left column.

A. WMAP + priors

As one might have expected, the inclusion of WMAP data is crucial for finding a good neutrino mass limit. The upper limit from WMAP data alone found here, $M_\nu < 1.75\text{eV}$, resides between the former results found by the WMAP team for their 3 year data, $M_\nu < 2.0\text{eV}$ [14], and the results from ref. [16] using the same data with a modified likelihood code, $M_\nu < 1.57\text{eV}$. In this case we see that both a CMF and HST prior will help significantly in constraining M_ν , and adding the CMF prior to the WMAP data yields an upper bound of $M_\nu < 1.43\text{eV}$.

The CMF prior put constraints on a combination of Ω_m and σ_8 , and in Figure 2 we show confidence contours in the plane of M_ν and $\sigma_8(\Omega_m/0.3)^{0.37}$ from WMAP data only, and when we add the CMF prior. It is well known that there is a positive correlation between M_ν and Ω_m in the CMB power spectrum. Both these parameters will alter the amplitudes of the CMB peaks, by shifting the time of matter-radiation equality. At this time neutrinos in this mass range were still relativistic, and contributed to the radiation part. Keeping Ω_m constant and increasing f_ν will thus postpone the time of matter-radiation equality and therefore enhance the amplitude of the acoustic peaks. To shift the time of equality back and lower the acoustic peaks, one has to increase Ω_m correspondingly. However, the effective parameter from the

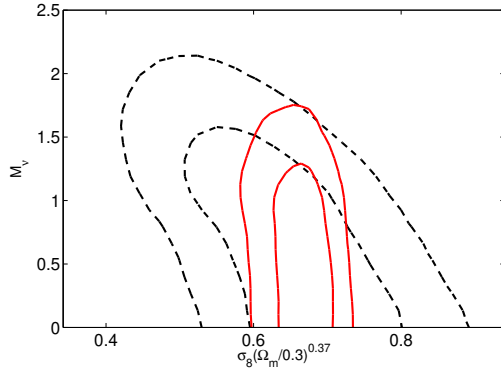


FIG. 2: 68% and 95% C.L. contours in the plane of M_ν and the effective parameter from the CMF constraint, $\sigma_8(\Omega_m/0.3)^{0.37}$. The dashed black line shows the contours when using WMAP data only, and the solid black lines show the results when adding the prior from the CMF.

CMF constraint, $\sigma_8(\Omega_m/0.3)^{0.37}$, also contains the amplitude parameter σ_8 which is negatively correlated with M_ν (from the same reasoning). From Figure 2 we see that this negative correlation is strong enough to make also the correlation between M_ν and $\sigma_8(\Omega_m/0.3)^{0.37}$ negative; that is, small values of $\sigma_8(\Omega_m/0.3)^{0.37}$ favor a large neutrino mass. When we add the CMF prior the allowed region of low values of $\sigma_8(\Omega_m/0.3)^{0.37}$ shrinks, and the upper limit on M_ν is reduced correspondingly.

Note that with this limit ($M_\nu < 1.43$ eV) we have not used any LSS or SNIa data, or any other prior on H_0 or Ω_b . We therefore claim this neutrino mass limit to be robust.

B. Including large scale structure

When adding LSS data the neutrino mass limit improves significantly, giving $M_\nu < 1.02$ eV for WMAP+2dF and $M_\nu < 1.05$ eV for WMAP+SDSS. However, when adding the CMF prior, a strange effect occurs. While this improves the M_ν limit to $M_\nu < 0.89$ eV in the case of WMAP+2dF, the limit increases to $M_\nu < 1.13$ eV with WMAP+SDSS. This may indicate a inconsistency between the CMF prior and SDSS. In Figure 3 we show the marginalized distribution of the $\sigma_8(\Omega_m/0.3)^{0.37}$ parameter when using WMAP, WMAP+CMF, WMAP+2dF, WMAP+SNLS or WMAP+SDSS. For the latter, the distribution deviates significantly from the four former, and we see that the WMAP+SDSS data set prefers larger values of $\sigma_8(\Omega_m/0.3)^{0.37}$ than the other combinations. This is in good accordance with the results obtained in ref. [30], where they found that WMAP+SDSS preferred larger values for both Ω_m and σ_8 than what was found with WMAP alone or WMAP+2dF (using the WMAP 1-year data). Figure 3 indicates that we should be careful when

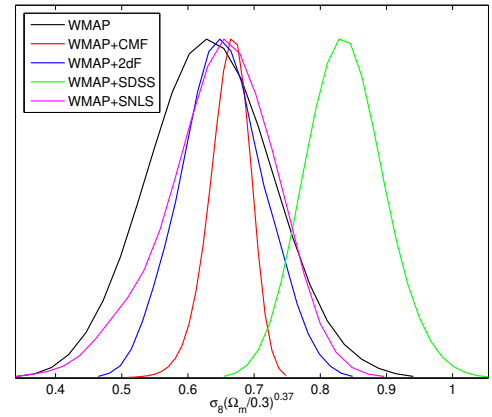


FIG. 3: Marginalized one-dimensional distribution of $\sigma_8(\Omega_m/0.3)^{0.37}$ when using WMAP data (black line), WMAP+CMF (red line), WMAP+2dF (blue line), WMAP+SDSS (green line) and WMAP+SNLS (purple line).

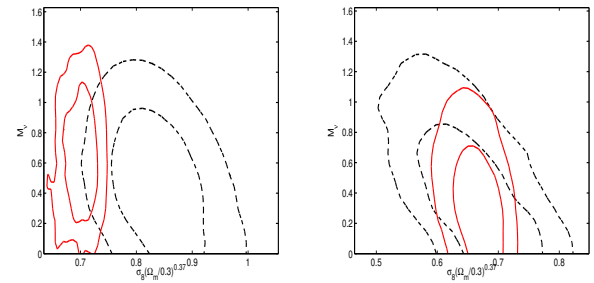


FIG. 4: 68% and 95% C.L. contours in the plane of $\sigma_8(\Omega_m/0.3)^{0.37}$ and M_ν . Left panel: Contours from WMAP+SDSS (black, dashed line), and WMAP+SDSS+CMF (red, solid line). Right panel: Contours from WMAP+2dF (black, dashed line), and WMAP+2dF+CMF (red, solid line).

using data from SDSS in combination with 2dF or CMF. Doing this, the inconsistencies may produce artificially narrow parameter distributions. In our case, the result of using WMAP+SDSS+CMF is that we not only get an upper limit on M_ν , but also a lower limit, such that our 95% C.L. limit becomes 0.23 eV $< M_\nu < 1.13$ eV for this combination of data sets. In Figure 4 we show the confidence contours in the plane of $\sigma_8(\Omega_m/0.3)^{0.37}$ and M_ν for WMAP+2dF and WMAP+SDSS with and without the CMF prior. From these plots it is clear how the incompatibility of SDSS and CMF produces the lower limit on M_ν .

When adding LSS data to the WMAP data set, we see that the HST prior is still important to improve the M_ν limits, while the BBN prior is not needed.

Also, it is interesting to note that adding the BAO prior to the WMAP+2dF data set combination has es-

sentially no effect for the neutrino mass limits, whereas adding the BAO prior to the WMAP+SDSS data sets improves the neutrino mass limit by almost a factor two. Again this illustrates the differences between the 2dF and SDSS sample. The reason why the BAO prior is more important when using SDSS, is the larger preferred value of $\Omega_m h^2$ for the SDSS sample. Adding the BAO prior will constrain the allowed region of large $\Omega_m h^2$, and thus also the allowed space for large M_ν .

We have also tried to constrain M_ν using LSS data alone, resulting in mass limits of order $M_\nu \lesssim 6\text{eV}$. So although LSS data in principle is a sensitive probe for neutrino masses, one needs to add CMB data to break parameter degeneracies.

C. Including supernova data

The inclusion of supernova data turns out to be as important as LSS for constraining neutrino masses. Again, this can be understood by the M_ν - Ω_m degeneracy. SNIa data is an effective probe of the amount of dark energy in the universe, and under the flatness assumption this will also automatically constrain Ω_m . In Figure 3 we see that also the data set combination WMAP+SNLS seems to be consistent with WMAP alone, WMAP+2dF and CMF prior, whereas it seems to be in some tension with SDSS data. In the case of WMAP+SNLS we see from Table I that adding the CMF prior improves the neutrino mass limit significantly, and that the inclusion of the CMF prior is a lot more constraining for neutrino masses than both the HST and BBN prior in this case. This means that if one believes in the SNIa measurements, we have an upper limit of $M_\nu < 0.70\text{eV}$ without using LSS measurements at all.

Note also that we can get a neutrino mass limit as low as $M_\nu < 0.40\text{eV}$ without using Ly- α data, if we combine WMAP+SNLS+SDSS+BAO+HST. But this limit weakens to $M_\nu < 0.79\text{eV}$ by substituting SDSS with 2dF. Again, this illustrates how sensitive the neutrino mass limit is to the choice of LSS sample and combination of priors.

V. CONCLUSION

In this paper we have studied cosmological neutrino mass limits, and how sensitive these limits are to different choices of data sets and priors. We have also included a new prior from the cluster mass function measured by weak gravitational lensing, which is a direct probe of the total mass distribution in the universe.

We report neutrino mass limits using 48 different combinations of data sets and priors, and we find that the neutrino mass limit is very sensitive to small changes in combinations of data sets and priors. Especially striking results are found when interchanging data sets between the SDSS and 2dF galaxy surveys. For example will the combination WMAP+SDSS+BAO give $M_\nu < 0.52\text{eV}$ at 95% C.L., while WMAP+2dF+BAO gives $M_\nu < 0.97\text{eV}$. These discrepancies occur because of a slight inconsistency between the SDSS data and many of the other data sets used here, and combining inconsistent data sets may lead to unreliable results. Also, the inconsistencies between the two galaxy surveys indicate that there may be systematics related to e.g. the scale dependence of the bias parameter that have to be better understood before we can rely fully on the LSS data. By discarding these data sets, and in addition refraining from using constraints from SNIa, HST, and BBN, we end up with a conservative, although robust cosmological neutrino mass limit of $M_\nu < 1.43\text{eV}$ from using only WMAP data in combination with the CMF prior.

Acknowledgments

OE, JRK and HD acknowledge support from the Research Council of Norway through project numbers 159637, 162830 and 165491. Some of the results in this work are based on observations made with the Nordic Optical Telescope, operated on the island of La Palma jointly by Denmark, Finland, Iceland, Norway, and Sweden, in the Spanish Observatorio del Roque de los Muchachos of the Instituto de Astrofísica de Canarias.

- [1] M. Maltoni, T. Schwetz, M. A. Tortola, and J. W. F. Valle, *New J. Phys.* **6**, 122 (2004), hep-ph/0405172.
- [2] G. L. Fogli et al. (2006), hep-ph/0608060.
- [3] K. Eitel, *Nucl. Phys. Proc. Suppl.* **143**, 197 (2005).
- [4] S. R. Elliott and P. Vogel, *Ann. Rev. Nucl. Part. Sci.* **52**, 115 (2002), hep-ph/0202264.
- [5] A. Goobar, S. Hannestad, E. Mortsell, and H. Tu (2006), astro-ph/0602155.
- [6] U. Seljak, A. Slosar, and P. McDonald (2006), astro-ph/0604335.
- [7] J. Lesgourgues and S. Pastor, *Phys. Rept.* **429**, 307 (2006), astro-ph/0603494.
- [8] C. Zunckel and P. G. Ferreira (2006), astro-ph/0610597.
- [9] S. Hannestad, *Phys. Rev. Lett.* **95**, 221301 (2005), astro-ph/0505551.
- [10] K. Ichikawa and T. Takahashi (2005), astro-ph/0510849.
- [11] A. De La Macorra, A. Melchiorri, P. Serra, and R. Bean (2006), astro-ph/0608351.
- [12] J.-Q. Xia, G.-B. Zhao, and X. Zhang (2006), astro-ph/0609463.
- [13] K. Ichikawa, M. Fukugita, and M. Kawasaki, *Phys. Rev. D* **71**, 043001 (2005), astro-ph/0409768.
- [14] D. N. Spergel et al. (2006), astro-ph/0603449.
- [15] M. Fukugita, K. Ichikawa, M. Kawasaki, and O. Lahav, *Phys. Rev. D* **74**, 027302 (2006), astro-ph/0605362.
- [16] J. R. Kristiansen, H. K. Eriksen, and O. Elgaroy (2006),

astro-ph/0608017.

[17] S. Cole et al. (The 2dFGRS), *Mon. Not. Roy. Astron. Soc.* **362**, 505 (2005), astro-ph/0501174.

[18] M. Tegmark et al. (SDSS), *Phys. Rev. D* **69**, 103501 (2004), astro-ph/0310723.

[19] W. J. Percival et al. (2006), astro-ph/0608636.

[20] R. E. Smith, R. Scoccimarro, and R. K. Sheth (2006), astro-ph/0609547.

[21] A. Refregier, *Annual Review of Astronomy & Astrophysics* **41**, 645 (2003), astro-ph/0307212.

[22] P. Schneider, in *Saas-Fee Advanced Course 33: Gravitational Lensing: Strong, Weak and Micro*, edited by G. Meylan, P. Jetzer, P. North, P. Schneider, C. S. Kochanek, and J. Wambsganss (2006), pp. 269–451.

[23] G. M. Voit, *Reviews of Modern Physics* **77**, 207 (2005), astro-ph/0410173.

[24] H. Dahle (2006), astro-ph/0608480.

[25] G. Mangano et al., *Nucl. Phys. B* **729**, 221 (2005), hep-ph/0506164.

[26] G. Hinshaw et al. (2006), astro-ph/0603451.

[27] H. K. Eriksen et al. (2006), astro-ph/0606088.

[28] K. M. Huffenberger, H. K. Eriksen, and F. K. Hansen (2006), astro-ph/0606538.

[29] M. Tegmark et al. (SDSS), *Astrophys. J.* **606**, 702 (2004), astro-ph/0310725.

[30] A. G. Sanchez et al., *Mon. Not. Roy. Astron. Soc.* **366**, 189 (2006), astro-ph/0507583.

[31] S. Cole, A. G. Sanchez, and S. Wilkins (2006), astro-ph/0611178.

[32] P. Astier et al., *Astron. Astrophys.* **447**, 31 (2006), astro-ph/0510447.

[33] E. Rasia, S. Ettori, L. Moscardini, P. Mazzotta, S. Borgani, K. Dolag, G. Tormen, L. M. Cheng, and A. Di aferio, *Mon. Not. Roy. Astron. Soc.* **369**, 2013 (2006), astro-ph/0602434.

[34] H. Dahle, N. Kaiser, R. J. Irgens, P. B. Lilje, and S. J. Maddox, *Astrophys. J. Suppl.* **139**, 313 (2002).

[35] R. K. Sheth and G. Tormen, *Mon. Not. Roy. Astron. Soc.* **308**, 119 (1999), astro-ph/9901122.

[36] W. L. Freedman et al., *Astrophys. J.* **553**, 47 (2001), astro-ph/0012376.

[37] S. Burles, K. M. Nollett, and M. S. Turner, *Phys. Rev. D* **63**, 063512 (2001), astro-ph/0008495.

[38] G. Steigman, *Int. J. Mod. Phys. E* **15**, 1 (2006), astro-ph/0511534.

[39] A. Blanchard, M. Douspis, M. Rowan-Robinson, and S. Sarkar, *Astron. Astrophys.* **412**, 35 (2003), astro-ph/0304237.

[40] A. Sandage et al. (2006).

[41] D. J. Eisenstein et al., *Astrophys. J.* **633**, 560 (2005), astro-ph/0501171.

[42] A. Lewis and S. Bridle, *Phys. Rev. D* **66**, 103511 (2002), astro-ph/0205436.

[43] <http://lambda.gsfc.nasa.gov>; version v2p2p1.